ACS Catalysis

Letter

pubs.acs.org/acscatalysis

Composition-Dependent Catalytic Activity of Bimetallic Nanocrystals: AgPd-Catalyzed Hydrodechlorination of 4-Chlorophenol

Hongpan Rong,[†] Shuangfei Cai,[†] Zhiqiang Niu,*[,†] and Yadong Li*[,†,‡]

[†]Department of Chemistry, Tsinghua University, Beijing, 100084, People's Republic of China

[‡]Department of Chemistry and the State Key Laboratory of Low-Dimensional Quantum Physics, Tsinghua University, Beijing, 100084, People's Republic of China

Supporting Information

ABSTRACT: Ag−Pd bimetallic nanocrystals (NCs) with tunable compositions and narrow size distributions were produced by a one-pot synthesis. The NC growth process was investigated by time-dependent TEM, XRD, and UV−vis studies. In the hydrodechlorination of 4-chlorophenol, the $AgPd_x$ (x = 2, 4, 6, 9, 19) showed pronounced composition-dependent catalytic activities, leading to the $AgPd_9$ catalyst with excellent activity.

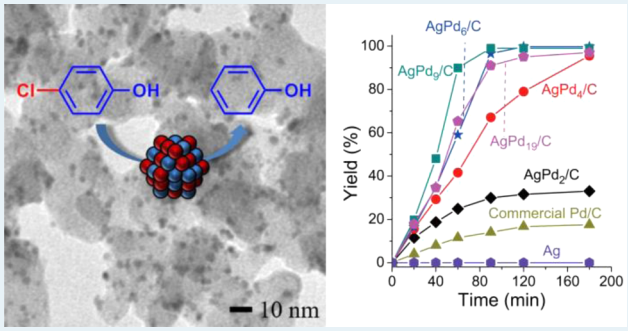

KEYWORDS: *Ag, Pd, nanocrystals, hydrodechlorination*

Precious metals are widely used in chemical engineering. Recently, bimetallic NCs, such as Pt-based[1−6] and Pd-based[7−12] nanostructures, have attracted tremendous research interest due to their better catalytic properties than monometallic NCs. Previous studies have shown that the catalytic performance of bimetallic NCs has a close relationship with their composition because the relative amount of each constituent metal could tune the electronic state of the primary catalytically active component.[13,14]

Chlorophenols (CPs) are widely present in waste waters of paper, dyes, pesticides, textiles, and petrochemicals.[15,16] Because of the stability of the chlorine−carbon bonds, CPs are difficult to biodegrade. Thus, to develop mild methods for dechlorination of CPs is of great importance. Compared with other precious metal catalysts from group VIII (Ru, Rh, and Pt), Pd has a better performance in the hydrodechlorination (HDC) reaction and lower cost.[17−22] For instance, Pd−Ag sol−gel catalyzed 1,2-dichloroethane to ethylene was carefully studied by Heinrichs and co-workers.[23−26] Similar catalysts ($Pd-Ag/SiO_2$ and $Pd-Cu/SiO_2$ cogelled xerogel catalysts) used for the same reaction have been reported by Lambert and co-workers.[22] Although systematic investigations of HDC process have been performed in these studies, the synthesis method of the xerogel $Pd-Ag/SiO_2$ was somewhat complicated, which included drying under vacuum, calcination, and reduction. Therefore, the facile synthesis of monodispersed Ag−Pd NCs and investigation of their properties toward HDC reactions under mild conditions are of significance.

Herein, we prepared narrowly distributed $AgPd_x$ NCs with tunable compositions and investigated their growth mechanism by time-dependent TEM, XRD, and UV−vis studies. The as-prepared monodispersed $AgPd_x$ NCs were deposited on carbon black and performed high catalytic activity for the HDC reaction at room temperature and atmospheric pressure. A pronounced composition-dependent activity trend was established in the HDC reaction, and the $AgPd_9/C$ catalysts showed the highest catalytic activity among all $AgPd_x$ NCs/C.

The $AgPd_x$ NCs were synthesized by coreduction of $AgNO_3$ and $Pd(acac)_2$ in octadecylamine (see details in the Supporting Information). Figure 1 depicts the TEM images of as-prepared $AgPd_x$ NCs. By varying the ratios of $AgNO_3$ and $Pd(acac)_2$, the compositions of $AgPd_x$ (x = 2, 4, 6, 9, 19) NCs could be finely tuned while their sizes remained in the range of 3−5 nm. When $AgNO_3$ was the only precursor, Ag NCs of (11.9 ± 1.4) nm (Supporting Information Figure S1a) were obtained; when $Pd(acac)_2$ was the only precursor, Pd NCs of (7.5 ± 1.7) nm were produced (Supporting Information Figure S1b). A representative high-resolution (HR) TEM image of the $AgPd_4$ NCs (Supporting Information Figure S2) shows that the products exhibit good crystallinity and the interplanar spacings of lattice fringes are 0.23 nm. The XRD patterns of the as-obtained $AgPd_x$ NCs are shown in Figure 1f. The diffraction peaks positioned between the standard peaks of Ag (JCPD-65-

Received: January 28, 2013
Revised: June 5, 2013
Published: June 10, 2013

   dx.doi.org/10.1021/cs400282a | *ACS Catal.* 2013, 3, 1560−1563

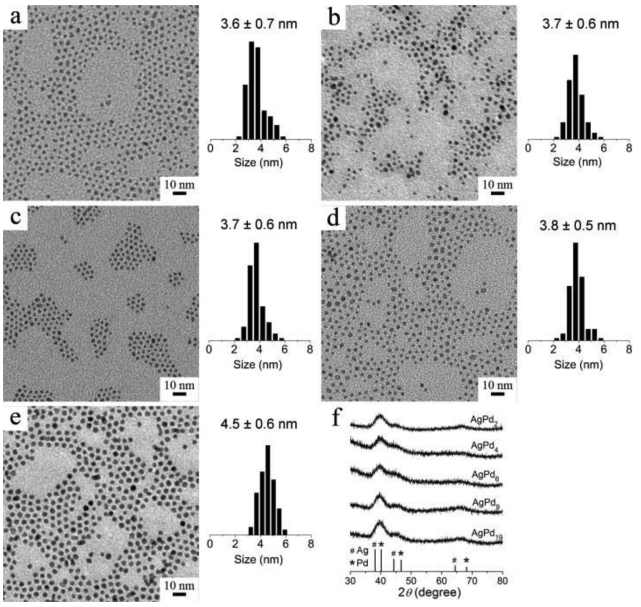

Figure 1. TEM images of as-prepared (a) $AgPd_2$, (b) $AgPd_4$, (c) $AgPd_6$, (d) $AgPd_9$, and (e) $AgPd_{19}$ NCs and (f) their corresponding XRD patterns.

6174) and Pd (JCPD-65-2871), demonstrating the formation of the bimetallic phase of Ag and Pd. As expected, with an increase in the Pd content, the peaks continuously shifted from Ag standard peaks to Pd. The exact atomic ratios of the $AgPd_x$ NCs were determined by energy dispersive X-ray (EDX) spectroscopy (Supporting Information Figure S3) and inductively coupled plasma–atomic emission spectroscopy (ICP–AES; Supporting Information Table S1), which is almost identical to that of the precursors. This observation indicates the atomic ratio of the products could be effectively controlled by the addition content of the precursors.

The nature of the particle surface was studied by Fourier transform infrared (FT-IR) spectra and X-ray photoelectron spectroscopy (XPS). Supporting Information Figure S4 shows the FT-IR spectra of as-prepared Pd, $AgPd_4$, and Ag NCs. The peaks around 3440 and 1630 cm^{-1} of Pd, $AgPd_4$, and Ag NCs were assigned to the N–H stretch and N–H scissor, respectively. These two peaks shifted to higher wavenumbers compared with pure octadecylamine, indicating the interaction of NCs with the nitrogen atoms of residual capping ligands. The $AgPd_x$ NCs were further characterized by XPS. A slight enrichment of silver on the surface of $AgPd_x$ NCs was observed (Supporting Information Table S1). The surface compositions of $AgPd_2$, $AgPd_4$, $AgPd_6$, $AgPd_9$, and $AgPd_{19}$ were determined to be $Ag_{1.7}Pd_2$, $Ag_{1.3}Pd_4$, $Ag_{1.3}Pd_6$, $Ag_{1.2}Pd_9$, and $Ag_{1.7}Pd_{19}$, respectively. As shown in Figure 2, the binding energies of the Ag $3d_{5/2}$ lie in the range of 367.6–367.7 eV, which are lower (about 0.6 eV) than the bulk Ag (368.2 eV). The Pd $3d_{5/2}$ binding energies obtained from $AgPd_x$ (x = 19, 9, 6) are very near the value of bulk Pd (335.4 eV); however, when the atomic ratio of Ag/Pd further was increased to 1/4 and 1/2, the Pd $3d_{5/2}$ binding energies exhibited negative shifts of 0.2 and 0.4 eV, respectively. The negative core level shifts relative to bulk Ag and Pd could be ascribed to the increase in the charge density in the d band with a loss in the sp band.[27]

The formation process of $AgPd_x$ NCs was investigated through time-dependent TEM, XRD, and UV–vis studies by using $AgPd_4$ as a model system. Figure 3a–d displays a series of

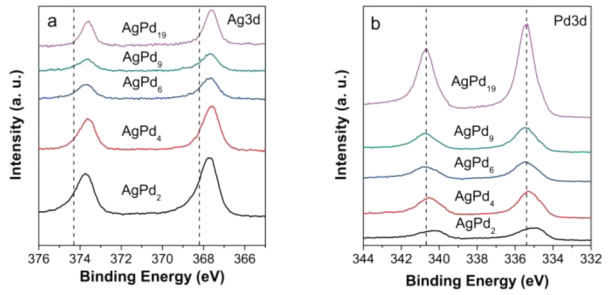

Figure 2. XPS spectra of the (a) Ag 3d and (b) Pd 3d regions for the $AgPd_x$ NCs.

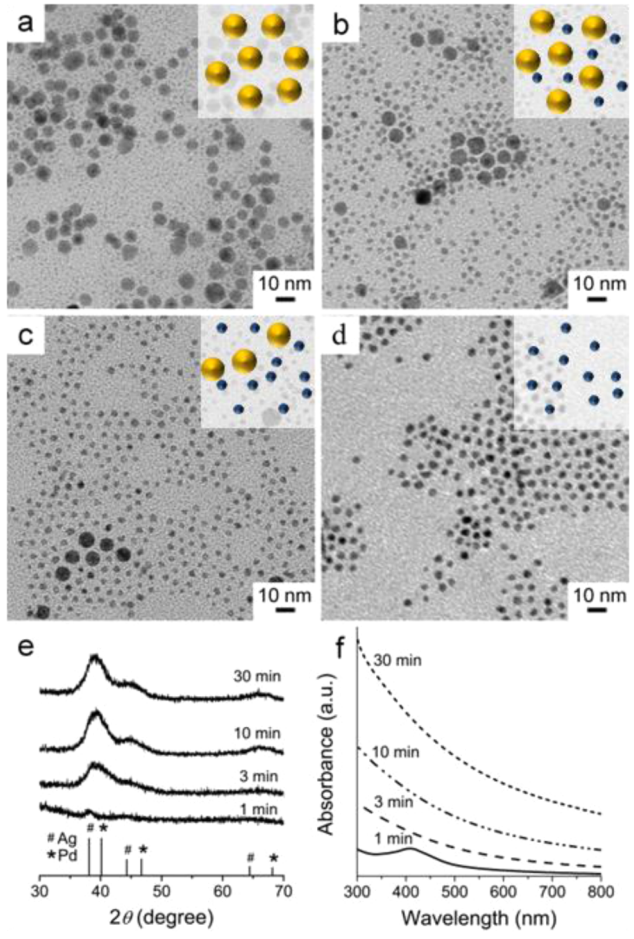

Figure 3. TEM images of $AgPd_4$ NCs obtained at different reaction times: (a) 1, (b) 3, (c) 10, and (d) 30 min. (e) XRD patterns and (f) UV–vis spectra of the products obtained from different reaction times.

typical TEM images of products obtained at different reaction times in the preparation of $AgPd_4$.[28] In a 1 min reaction, most of the products were 10 nm NCs (Figure 3a). As the reaction proceeded, the 10 nm NCs gradually disappeared while more and more 4 nm NCs appeared (3–10 min, Figure 3c–d). In a 30 min reaction, all the products evolved to 4 nm NCs. Figure 3e and f shows the corresponding XRD patterns and absorption spectra of the samples shown in Figure 3a–d, respectively. The products collected in a 1 min reaction are mainly Ag NCs, as indicated by the XRD and characteristic SPR (surface plasma resonance) band at 409 nm observed in the absorption spectrum. Thereafter (3–30 min), the characteristic SPR peak of Ag disappeared, and the XRD patterns shifted to higher 2θ

dx.doi.org/10.1021/cs400282a | ACS Catal. 2013, 3, 1560–1563

degree, indicating the Ag−Pd alloy formed at the consumption of Ag NCs. The chemical process observed in the growth of $AgPd_4$ could be attributed to galvanic replacement of Ag with Pd.[29]

The as-prepared $AgPd_x$ NCs were then supported on carbon black and submitted to the HDC reaction under mild conditions (room temperature and atmosphere pressure). First, $AgPd_4$/C (Supporting Information Figure S5) was used as a probe catalyst to screen the best reaction conditions in the HDC of 4-chlorophenol. Previous studies revealed that the HCl formed during the reaction could poison the Pd and decrease the reaction rate.[30] Therefore, neutralizer is necessary, and we used NaOH as the base to test different solvents (Table 1, entries 1−7). The yields of phenol in dimethyl sulfoxide (DMSO), methanol, 1,4-dioxane, H_2O, *N*,*N*-dimethylformamide (DMF), toluene, and tetrahydrofuran (THF) were 0, 14%, 47%, 51%, 60%, 66%, and 99%, respectively. Different bases were also tested in the THF system (Table 1, entries 7−10). It shows that the yield of the HDC reaction is greatly affected by the basicity of neutralizer for HCl. When the neutralizer is a strong base (NaOH, KOH), the reaction equilibrium moves to the right, and the reaction rate is high. In contrast, the reaction rate is sluggish when the base is weak ($NaCO_3$, CH_3CH_2COONa).

Table 1. Effect of Different Solvents and Different Bases[a]

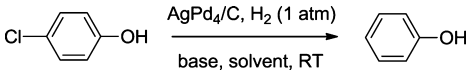

entry	base	solvent	yield (%)[b]
1	NaOH	DMSO	0
2	NaOH	CH_3OH	14
3	NaOH	1,4-dioxane	47
4	NaOH	H_2O	51
5	NaOH	DMF	60
6	NaOH	toluene	66
7	NaOH	THF	99
8	KOH	THF	98
9	Na_2CO_3	THF	10[c]
10	CH_3CH_2COONa	THF	27[c]

[a]Conditions: 4-chlorophenol (1 mmol, 128.6 mg), base (1.5 mmol), catalyst loading (0.6 mol % based on initial 4-chlorophenol), solvent (3 mL), *n*-tridecane (0.3 mmol), H_2 balloon, 25 °C, 4 h. [b]Determined by GC. [c]Reaction time was prolonged to 24 h.

Using THF and NaOH as the optimal solvent and base, we explored the role of Pd and Ag in the HDC reaction. Figure 4a shows the yield of phenol versus time during the HDC reaction catalyzed by different catalysts. Not surprisingly, Ag nanoparticle (11.9 nm, Supporting Information Figure S2a) was inactive, indicating Pd is the intrinsic active sites for the HDC reaction.[25,26] Meanwhile, as the benchmark catalysts, commercial Pd/C (Figure 4a) was found to be inferior to the $AgPd_x$ NCs/C catalysts, implying the promoting role of Ag in the HDC reaction. Moreover, the atomic ratio of Ag/Pd was found to have a pronounced influence over the activity of the $AgPd_x$ NCs/C catalysts. As displayed in Figure 4b, the turnover frequencies (TOFs) of $AgPd_x$ NCs/C catalysts showed a typical volcano curve: it initially improved along with the increase in Pd ($x < 9$) until it reached a peak value at 322 h^{-1}, then it dropped when more Pd was added. According to Sinfelt's report, Ag is able to absorb the chlorinated molecules and break

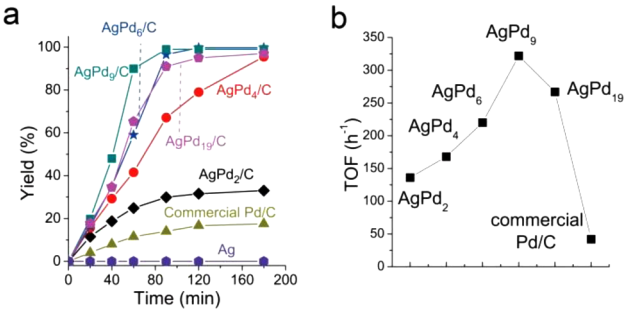

Figure 4. (a) The yield of phenol versus time during the HDC reaction catalyzed by different $AgPd_x$ NCs/C and (b) TOFs in the first hour for the HDC reaction of 4-chlorophenol. Conditions: 4-chlorophenol (1 mmol, 128.6 mg), base (1.5 mmol, 60.0 mg), catalyst loading (0.6 mol % based on initial 4-chlorophenol), THF (3 mL), *n*-tridecane (0.3 mmol), H_2 balloon, 25 °C, 3 h.

the C−Cl bond.[31] In the dechlorination of 1,2-dichloroethane on Ag−Pd/SiO_2, Heinrichs and co-workers found that chlorides first formed on the Ag surface from 1,2-dichloroethane, followed by a HDC process triggered by hydrogen adsorbed on Pd.[25,26] Considering the addition of Ag promoted the HDC reaction of 4-chlorophenol, as observed in this work, a sound mechanism was proposed as follows: 4-chlorophenol first absorbs on the surface of the $AgPd_x$ NCs, and the breaking of C−Cl bond occurs on the Ag sites. H atoms supplied via the dissociation of H_2 on Pd sites facilitate the HDC reaction and render the regeneration of metallic Ag from chlorinated silver (Supporting Information Figure S6).

In conclusion, narrowly distributed $AgPd_x$ NCs with controllable compositions have been prepared through a facile method. The as-prepared NCs performed well in a HDC reaction of 4-chlorophenol into phenol under mild conditions (room temperature and atmospheric pressure), and a pronounced composition-dependent catalytic activity of $AgPd_x$ NCs/C in this reaction was observed, which further prompts us to develop optimal bimetallic nanocatalysts with improved activities. We envision such a rational approach could be extended to other novel heterogeneous catalysts.

■ ASSOCIATED CONTENT

Supporting Information

Experimental details, HRTEM image of $AgPd_4$ NCs, TEM images of as-prepared Ag and Pd NCs, ICP and XPS results, effects of different solvents, EDX spectroscopy of as-prepared $AgPd_x$ NCs, TEM image of $AgPd_4$ supported on carbon black, TOF calculation details. This material is available free of charge via the Internet at http://pubs.acs.org.

■ AUTHOR INFORMATION

Corresponding Author

*E-mail: (Z.N.) zqniu@mail.tsinghua.edu.cn, (Y.L.) ydli@mail.tsinghua.edu.cn.

Notes

The authors declare no competing financial interest.

■ ACKNOWLEDGMENTS

This work was supported by the State Key Project of Fundamental Research for Nanoscience and Nanotechnology (2011CB932401 and 2011CBA00500), National Key Basic Research Program of China (2012CB224802), and the National Natural Science Foundation of China (Grants Nos.

20921001 and 21131004). We are grateful for helpful discussions and suggestions from Prof. Wei He (Tsinghua University).

■ ABBREVIATIONS

NCs, nanocrystals; CPs, chlorophenols; HDC, hydrodechlorination; XRD, X-ray diffraction; EDX, energy dispersive X-ray; ICP−AES, inductively coupled plasma−atomic emission spectroscopy; XPS, X-ray photoelectron spectroscopy; SPR, surface plasma resonance; THF, tetrahydrofuran; TOF, turnover frequency

■ REFERENCES

(1) Niu, Z. Q.; Wang, D. S.; Yu, R.; Peng, Q.; Li, Y. D. *Chem. Sci.* **2012**, *3*, 1925−1929.
(2) Hong, J. W.; Kang, S. W.; Choi, B.-S.; Kim, D.; Lee, S. B.; Han, S. W. *ACS Nano* **2012**, *6*, 2410−2419.
(3) Wang, D. S.; Zhao, P.; Li, Y. D. *Sci. Rep.* **2011**, *1*, 37.
(4) Wu, J. B.; Yang, H. *Nano Res.* **2011**, *4*, 72−82.
(5) Lim, B.; Jiang, M.; Yu, T.; Camargo, P. H. C.; Xia, Y. N. *Nano Res.* **2010**, *3*, 69−80.
(6) Yu, X. F.; Wang, D. S.; Peng, Q.; Li, Y. D. *Chem. Commun.* **2011**, 8094−8096.
(7) Niu, Z. Q.; Peng, Q.; Zhuang, Z. B.; He, W.; Li, Y. D. *Chem.—Eur. J.* **2012**, *18*, 9813−9817.
(8) Wu, Y. E.; Wang, D. S.; Zhao, P.; Niu, Z. Q.; Peng, Q.; Li, Y. D. *Inorg. Chem.* **2011**, *50*, 2046−2048.
(9) Yin, Z.; Zhou, W.; Gao, Y. J.; Ma, D.; Kiely, C. J.; Bao, X. H. *Chem.—Eur. J.* **2012**, *18*, 4887−4893.
(10) Yang, C. W.; Chanda, K.; Lin, P. H.; Wang, Y. N.; Liao, C. W.; Huang, M. H. *J. Am. Chem. Soc.* **2011**, *133*, 19993−20000.
(11) Xu, J.; Wilson, A. R.; Rathmell, A. R.; Howe, J.; Chi, M.; Wiley, B. J. *ACS Nano* **2011**, *5*, 6119−6127.
(12) Chang, S. H.; Su, W. N.; Yeh, M. H.; Pan, C. J.; Yu, K. L.; Liu, D. G.; Lee, J. F.; Hwang, B. J. *Chem.—Eur. J.* **2010**, *16*, 11064−11071.
(13) Zhang, J.; Yang, H.; Fang, J.; Zou, S. *Nano Lett.* **2010**, *10*, 638−644.
(14) Mazumder, V.; Chi, M.; More, K. L.; Sun, S. *J. Am. Chem. Soc.* **2010**, *132*, 7848−7849.
(15) Nair, A.; Pillai, M. K. K. *Sci. Total Environ.* **1992**, *121*, 145−157.
(16) Graham, L. J.; Atwater, J. E.; Jovanovic, G. N. *AIChE J.* **2006**, *52*, 1083−1093.
(17) Arcadi, A.; Cerichelli, G.; Chiarini, M.; Vico, R.; Zorzan, D. *Eur. J. Org. Chem.* **2004**, *2004*, 3404−3407.
(18) Babu, N. S.; Lingaiah, N.; Prasad, P. S. S. *Appl. Catal., B* **2012**, *111*, 309−316.
(19) Diaz, E.; Casas, J. A.; Mohedano, A. F.; Calvo, L.; Gilarranz, M. A.; Rodriguez, J. J. *Ind. Eng. Chem. Res.* **2008**, *47*, 3840−3846.
(20) Molina, C. B.; Pizarro, A. H.; Casas, J. A.; Rodriguez, J. J. *Water Sci. Technol.* **2012**, *65*, 653−660.
(21) Sun, C.; Wu, Z.; Mao, Y.; Yin, X.; Ma, L.; Wang, D.; Zhang, M. *Catal. Lett.* **2011**, *141*, 792−798.
(22) Lambert, S.; Ferauche, F.; Brasseur, A.; Pirard, J. P.; Heinrichs, B. *Catal. Today* **2005**, *100*, 283−289.
(23) Heinrichs, B.; Delhez, P.; Schoebrechts, J. P.; Pirard, J. P. *J. Catal.* **1997**, *172*, 322−335.
(24) Heinrichs, B.; Noville, F.; Schoebrechts, J. P.; Pirard, J. P. *J. Catal.* **2000**, *192*, 108−118.
(25) Heinrichs, B.; Schoebrechts, J. P.; Pirard, J. P. *J. Catal.* **2001**, *200*, 309−320.
(26) Heinrichs, B.; Noville, F.; Schoebrechts, J. P.; Pirard, J. P. *J. Catal.* **2003**, *220*, 215−225.
(27) Slanac, D. A.; Hardin, W. G.; Johnston, K. P.; Stevenson, K. J. *J. Am. Chem. Soc.* **2012**, *134*, 9812−9819.
(28) The reaction temperature was lowered to 170 °C, at which temperature the reaction speed was slower.
(29) Chen, J.; Wiley, B.; McLellan, J.; Xiong, Y.; Li, Z.-Y.; Xia, Y. *Nano Lett.* **2005**, *5*, 2058−2062.
(30) Aramendia, M. A.; Borau, V.; Garcia, I. M.; Jimenez, C.; Lafont, F.; Marinas, A.; Marinas, J. M.; Urbano, F. J. *J. Mol. Catal. A: Chem.* **2002**, *184*, 237−245.
(31) Fung, S. C.; Sinfelt, J. H. *J. Catal.* **1987**, *103*, 220−223.